SUSTAINABLE FLEXIBLE FILMS BASED ON NATURAL POLYSACCHARIDES USABLE AS NANOMATERIAL SUPPORT

[1,2]Jan BRAUN, [1,2]Sabrin ABDALLAH, [3,2]Ondřej HAVELKA, [1,2]Michal SALAVA, [4]Rafael TORRES-MENDIETA

[1]Institute for Nanomaterials, Advanced Technologies and Innovation, Technical University of Liberec, Studentská 1402/2, 461 17 Liberec, Czech Republic, EU, jan.braun@tul.cz

[2]Faculty of Mechatronics, Informatics and Interdisciplinary Studies, Technical University of Liberec, Studentská 1402/2, 461 17 Liberec, Czech Republic, EU

[3]Department of Chemistry, Technical University of Liberec, Studentská 1402/2, 461 17 Liberec, Czech Republic, EU

[4]Department of Chemical Sciences, University of Padua, Via Marzolo 1, 35131 Padova, Italy, EU, rafael.omar.torres.mendieta@gmail.com

https://doi.org/10.37904/nanocon.2025.5199

Abstract

The global push for eco-friendly and biodegradable alternatives to conventional plastics has intensified interest in natural polymers for sustainable functional materials. In this contribution, we present a robust formulation for highly sustainable, flexible composite films engineered from a synergistic combination of two abundant polysaccharides, carrageenan (CG) and sodium alginate (SA). These abundant biopolymers were selected for their intrinsic film-forming ability, non-toxicity, and biodegradability, offering a green alternative for advanced material design. Using a solvent-casting technique without toxic crosslinkers, we engineered CG-SA composite films with tailored structural and mechanical performance by modulating the CG:SA ratio.

A thorough investigation of the films' structural, thermal, optical, surface, and mechanical properties reveals a strong compositional dependence, with the most pronounced synergistic effect observed in mechanical performance. Notably, a CG:SA ratio of 40:60 permits a synergistic molecular interaction between the polysaccharides, enabling a fourfold increase in tensile strength and over twofold improvement in elongation at break compared to films made from single-component systems. Given their biodegradable nature, processability, and mechanical resilience, these films are strong candidates for supporting nanomaterials traditionally implemented in real-world applications such as eco-conscious food packaging using ZnO or nanoclays, in flexible electronics with carbon nanostructures, in wearable sensors employing plasmonic nanoparticles, or in bio-integrated substrates with polymer nanoparticles. This work, thus, contributes to the growing field of green nanomaterial supporting platforms, offering a scalable, non-toxic route aligned with the objectives of sustainable nanotechnology.

Keywords: Natural polysaccharides, carrageenan, sodium alginate, nanomaterial support, sustainable materials

1. INTRODUCTION

Plastic pollution is one of the most pressing environmental issues of the 21st century. Indeed, the global plastic production surged from 2 million tons in 1950 to an astonishing 380 million tons by 2015, with projections indicating that this trend will continue to rise each year [1]. A significant portion of this plastic is not properly disposed of, often ending up in landfills or oceans, and breaking down into microplastics [2]. This escalating crisis underscores the need for sustainable, biodegradable alternatives to petroleum-based plastics; materials

that can degrade more rapidly without compromising functionality. In this context, natural biopolymers, particularly those sourced from marine biomass, have emerged as promising candidates because of their renewable origins and tunable properties [3].

Among biopolymers, SA and CG have attracted particular interest. Both polysaccharides are abundant, biodegradable, non-toxic, and possess inherent film-forming abilities. Extracted from brown algae (SA) and red algae (CG), they have long been utilised in food and medical applications, attesting to their safety and versatility [4]. Nevertheless, each polymer faces limitations when used alone. SA-based films, while excellent oxygen barriers, often suffer from low water resistance and modest mechanical strength [5]. Conversely, CG films generally lack stability and strength unless modified with additives [6]. To overcome these drawbacks, researchers have increasingly explored composite films combining CG and SA [7]. This strategy leverages their complementary features to yield materials with improved mechanical integrity, elasticity, and environmental resistance, all achieved without relying on synthetic additives or harmful crosslinkers.

Despite this progress, relatively few studies have investigated CG–SA composites, which are especially appealing when used as multifunctional platforms for incorporating nanomaterials [8]. Such composites offer unique opportunities: the CG–SA matrix can effectively host functional nanofillers, such as nanoparticles (e.g., ZnO, CuS, and TiO_2) [9], or nanoclays [10], enabling the design of intelligent food packaging with enhanced antimicrobial, barrier, or heat-resistant properties. Nanoalloys, for instance, those composed of iron and bismuth, provide excellent photocatalytic activity [11], which can be stabilised within the polymeric network to prevent aggregation. Likewise, carbon nanostructures can be integrated into these films, creating sustainable substrates for green wearable electronics [12].

We present a scalable formulation of CG–SA composite films fabricated through solvent casting without toxic crosslinking agents. By systematically varying the CG:SA ratio, we demonstrate how composition governs the films' structural, thermal, and mechanical properties. The resulting materials preserve the intrinsic advantages of their natural polymer components, i.e., biodegradability, flexibility, and safety, while offering a scalable pathway for advanced functionalization, providing an eco-friendly platform for nanomaterial integration.

2. METHODOLOGY

Synthesis of flexible substrates. κ-CG (predominantly κ-CG with minor amounts of λ-CG, Sigma-Aldrich, USA) and SA (Sigma-Aldrich, USA) powders were separately dissolved in deionised water at a concentration of 1.5 % (w/v), which is often used in literature [13]. Each solution was magnetically stirred overnight to ensure complete dissolution. The CG and SA solutions were then combined in seven ratios (C-S: 100-0, 80-20, 60-40, 50-50, 40-60, 20-80, and 0-100) and stirred for an additional hour. To each 50 mL of the blended solution, 1 mL of glycerol (≥99.5%, Sigma-Aldrich, USA) was added as a plasticiser, followed by an additional 60 minutes of magnetic stirring to ensure homogeneity. Twenty millilitres of each film-forming solution was then cast into plastic Petri dishes and dried either in an oven at 40 °C for 8 hours or under ambient conditions to produce the CG–SA composite films.

Film characterisation. After drying, the films were subjected to comprehensive physicochemical characterisation. Cross-sectional morphology was examined using scanning electron microscopy (SEM; Helios 5 PFIB CXe DualBeam, Thermo Scientific, USA). Fourier transform infrared spectroscopy (FTIR; Nicolet iZ10, Thermo Scientific, USA) was performed to detect structural changes in the polymeric network. Optical transparency was assessed using ultraviolet–visible (UV–Vis) spectroscopy (Optima 2100Dv, Perkin Elmer). Thermal stability was analysed via thermogravimetric analysis (TGA; Q500, TA Instruments, USA) with a heating rate of 10 °C·min^{-1} to 600 °C in a synthetic air atmosphere (i.e., 80 % nitrogen, 20 % oxygen).

Mechanical testing. Mechanical properties, including tensile strength and elongation at break, were measured using a universal tensile tester (LabTest 6.0051, LaborTech, Czechia) equipped with a 10 N load cell (AST,

Germany; accuracy class 1 from 0.030 N and class 0.5 from 0.1 N, EN ISO 7500-1). For each CG–SA formulation, 10 strips (10 mm width) were cut from the dry films for testing.

The statistical evaluation of the mechanical experiments was executed by MATLAB R2024a software, and the normality of the data was assessed with the Kolmogorov-Smirnov test. Multiple group comparisons were conducted using the Kruskal-Wallis test followed by post hoc Dunn's test.

3. RESULTS AND DISCUSSION

3.1 SEM

Figure 1 shows a cross-sectional view of the CG-SA films, with an average thickness of 92.64 ± 1.36 µm. Clear structural differences are evident between CG- and SA-rich compositions. Films with higher SA content (C-S: 0-100, 20-80, and 40-60) display a uniformly ordered morphology, while those with increasing CG content (C-S: 60-40, 80-20, and 100-0) progressively lose this order as the proportion of SA decreases. The 50-50 film, where both components are present in equal amounts, appears to represent the critical composition at which internal order undergoes a marked transition, likely reflecting the distinct gelation mechanisms of CG and SA [14]. Such loss of order in low-SA films is undesirable, as it promotes microstructural irregularities that may act as light-scattering sites, ultimately reducing film transparency.

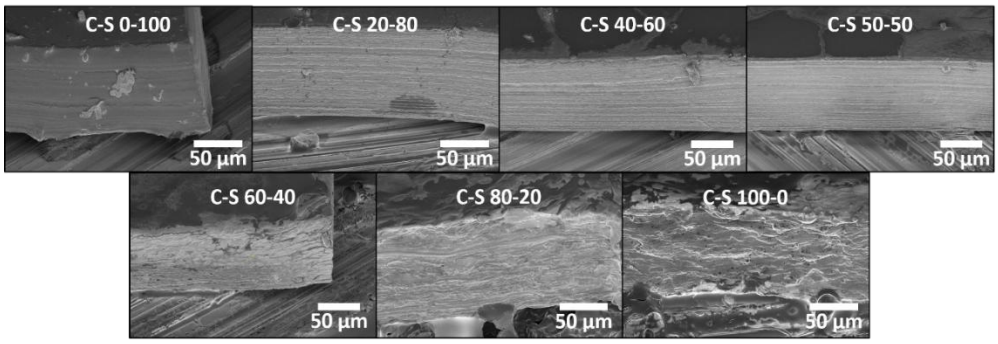

Figure 1 Representative SEM images showing the cross-section of individual CG-SA films

3.2 FTIR and UV-Vis spectroscopy

The FTIR spectra of individual CG–SA films are shown on the left side of **Figure 2**. Structural differences between CG and SA are most evident in the enlarged region from 1700 to 1150 cm^{-1}, where a gradual transition between the two polymers can be observed. In SA-rich samples, characteristic peaks appear at 1606 cm^{-1} and 1409 cm^{-1}, corresponding to symmetric and asymmetric COO^- vibrations, respectively. As CG content increases, the intensity of these COO^- peaks decreases, reflecting the absence of carboxylate groups in CG. Conversely, the characteristic CG peak at 1206 cm^{-1}, assigned to S=O stretching vibrations, diminishes with higher SA content due to the lack of sulphate groups in SA. Notably, an isosbestic point appears around 1267 cm^{-1}, where all spectra intersect, indicating the coexistence of both components in equilibrium and confirming the high quality of the binary mixtures [15].

Transparency measurements of the CG–SA films, shown on the right side of **Figure 2**, further support the microstructural trends anticipated in **Figure 1**. Films with higher SA content exhibit greater optical transmittance, consistent with their compact and ordered morphology that minimises defect density and scattering centres. In contrast, as predicted for low-SA films, increasing CG content introduces structural irregularities that serve as scattering and absorption sites, thereby reducing transparency. Together with the SEM findings, these results demonstrate that an ordered internal structure combined with an optimal thickness enables films to achieve high transparency while retaining sufficient mechanical robustness for practical handling without tearing.

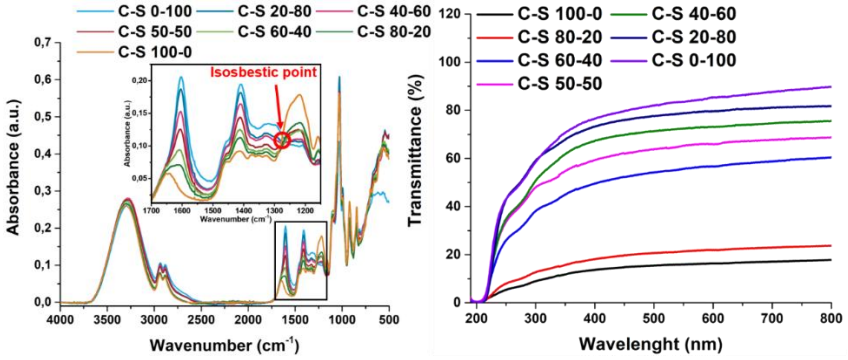

Figure 2 FTIR analysis of CG-SA films within the wave number range of 4000 to 500 cm^{-1}, with detail on the isobestic point area (left), UV-Vis spectra of films in the wavelength range from 180 to 800 nm showing transmittance of the CG-SA films (right)

3.3 Mechanical properties

As anticipated from the SEM and UV–Vis analyses, the mechanical testing results demonstrate that the composition of the films strongly influences both tensile strength and elongation at break (**Figure 3**). Interestingly, in contrast to the trend suggested by SEM, the lowest strength values were found in the single-component films: C-S: 100-0 (pure CG) and C-S: 0-100 (pure SA), with tensile strengths of 1.06 MPa and 0.83 MPa, respectively. The highest strength was observed in the composite C-S: 40-60 (4.75 MPa), closely followed by C-S: 60-40 (4.27 MPa) and C-S: 50-50 (4.19 MPa). These values are roughly four times greater than those of the pure materials. Moreover, the statistical analysis confirmed significant differences across most compositions, with the middle mixtures showing highly significant improvements ($p < 0.01$ to $p < 0.001$).

A similar pattern was observed for elongation at break. The mixed compositions, particularly C-S: 40-60 and C-S: 50-50, exhibited markedly higher elongation values (71.02 % and 62.71 %, respectively) compared to the pure CG (35.64 %) and SA (25.7 %) films. Thus, the composites nearly doubled the elongation capacity of the single-component samples. Moreover, the statistical analysis again confirmed significant differences between the mixed and pure films ($p < 0.01$ to $p < 0.001$).

These findings underscore the synergistic interaction between CG and SA, where, as anticipated by the formation of the isosbestic point revealed in FT-IR measurements, optimal dispersion of one polymer within the matrix of the other promotes efficient stress transfer and delays crack initiation. In contrast, the absence of such interfacial reinforcement in single-component films results in lower strength and reduced ductility. Together with the other analyses, these results highlight the effectiveness of controlled polymer blending in tuning both the transparency and the mechanical robustness of CG–SA films for specific application needs.

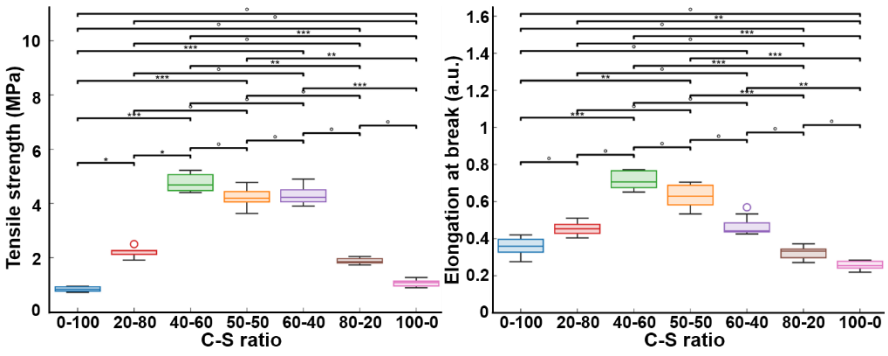

Figure 3 Box plots representing the obtained ultimate tensile strength and elongation at break for CG-SA films. The sign ° denotes no statistical significance, *, **, *** denote statistical significance at significance levels of 0.05, 0.01, and 0.001 (Kruskal-Wallis).

3.4 TGA

Beyond mechanical performance, the thermal degradation behaviour of the films further demonstrates their potential for technological applications. TGA revealed a multi-stage mass-loss profile that varied with composition. A low-temperature stage, corresponding to the evaporation of physically adsorbed or hydrogen-bonded water, appeared in most samples as small to medium derivative thermogravimetric (DTG) peaks between 50 and 63 °C for C-S: 100-0 (61.7 °C), 20-80 (61.2 °C), 60-40 (51.8 °C), 80-20 (62.7 °C), and 0-100 (50.9 °C) [16]. In contrast, no distinct moisture peak was observed for C-S: 40-60 and C-S: 50-50, whose first major decomposition events occurred directly at 176.1 °C and 172.8 °C, respectively. This absence suggests reduced retention of loosely bound water or overlap of water release with the onset of polymer and plasticiser volatilisation.

The dominant decomposition stage for all films occurred well above the safe operating limits of wearable and mobile devices, as defined in the SFS-EN IEC 62368-1:2020 standard [17] or food packaging [18], highlighting their suitability for such thermal-sensitive sectors. The main decomposition temperatures ranged from 170 to 190 °C, depending on composition. SA-rich systems such as C-S: 0-100 and C-S: 20-80 showed their most intense peaks at 170.9 °C and 176.6 °C, respectively, while CG-rich systems, including C-S: 100-0 (186.4 °C), 60-40 (185.5 °C), and 80-20 (188.8 °C) decomposed at slightly higher temperatures. This shift indicates that CG imparts greater thermal resistance than SA. In addition, secondary decomposition steps consistently appeared between 225 and 275 °C, corresponding to further breakdown of the polysaccharide backbone. Finally, at still higher temperatures (>350 °C), several samples exhibited additional degradation peaks, 343–417 °C and 516.9 °C for C-S: 100-0, 435–512 °C for 50-50, and 552 °C for 40-60, attributable to carbonisation and oxidation of stable residues [19].

Taken together, the TGA results confirm that film composition strongly governs thermal behaviour. Moreover, the absence of a distinct moisture event in C-S: 40-60 and 50-50 points to structural features that reduce water retention, while the lower main decomposition temperatures of SA-rich systems reflect their greater thermal lability. Conversely, the higher decomposition values and more persistent residues of CG-rich systems reveal their improved stability and char-forming capacity. When considered alongside the SEM, UV–Vis, FTIR, and tensile strength findings, these results identify C-S: 40-60 as the most promising candidate for a sustainable polymeric matrix, combining transparency, mechanical robustness, and thermal stability, for advanced applications such as food packaging and wearable devices development.

4. CONCLUSION

This study demonstrates a simple yet effective strategy for synthesising flexible and sustainable polysaccharide films from CG and SA in varying ratios, and systematically evaluating their physicochemical properties. By tailoring composition, the internal structure, optical transparency, mechanical strength, and thermal resistance of the films can be precisely modulated. Among the tested formulations, C-S: 40-60 emerged as the most promising candidate, showing clear evidence of synergistic molecular interactions between CG and SA. This composition achieved a fourfold increase in tensile strength and nearly doubled elongation at break compared with single-component films, while maintaining high transparency (>70% transmittance in the visible range) and exceptional thermal stability, with the first degradation event occurring at 176.1 °C, well above the overheating thresholds of up-and-coming thermally sensitive applications like food packaging and wearable electronics development. These combined properties position the C-S: 40-60 formulation as a practical and sustainable polymeric matrix for these advanced applications. Beyond establishing these structure–property relationships, this work lays the foundation for future studies on the integration of CG–SA composites with functional nanomaterials and carbon nanostructures, paving the way toward next-generation sustainable substrates with tailored multifunctionality.

ACKNOWLEDGEMENTS

This work was supported by the Student Grant Competition (SGS) at the Technical University of Liberec in 2025 under project No. SGS-2025-3527.

REFERENCES

[1] YAN, Huijie, et al. Future projections of global plastic pollution: scenario analyses and policy implications. *Sustainability*. 2024, vol. 16, no. 2.

[2] KIM, Min S., et al. A review of biodegradable plastics: chemistry, applications, properties, and future research needs. *Chemical Reviews*. 2023, vol. 123, no. 16.

[3] PRIYA, Bhanu, et al. Synthesis, characterization and antibacterial activity of biodegradable starch/pva composite films reinforced with cellulosic fibre. *Carbohydrate Polymers*. 2014, vol. 109, p. 171-179.

[4] BARANWAL, Jaya, et al. Biopolymer: a sustainable material for food and medical applications. *Polymers*. 2022, vol. 14, no. 5.

[5] ABDOLLAHI, Mehdi, et al. Reducing water sensitivity of alginate bio-nanocomposite film using cellulose nanoparticles. *International Journal of Biological Macromolecules*. 2013, vol. 54, p. 166-173.

[6] RAMADAS, Bharath K., et al. Recent progress of carrageenan-based composite films in active and intelligent food packaging applications. *Polymers*. 2024, vol. 16, no. 7.

[7] RIDLO, Ali, et al. Optimization and characterization of carrageenan/alginate ratio and seaweed waste to develop composite bioplastics from kappaphycus alvarezii. *Journal of Metals, Materials and Minerals*. 2025, vol. 35, no. 3.

[8] CIGALA, Rosalia M., et al. Biopolymeric nanocomposites for co2 capture. *Polymers*. 2024, vol. 16, no. 8.

[9] CHENG, Cheng, et al. Recent advances in carrageenan-based films for food packaging applications. *Frontiers in Nutrition*. 2022, vol. 9.

[10] KIA, Mahboubeh V., et al. Fabrication and characterization of transparent nanocomposite films based on poly (lactic acid)/polyethylene glycol reinforced with nano glass flake. *International Journal of Biological Macromolecules*. 2024, vol. 254, p. 127473.

[11] HAVELKA, Ondřej, et al. Laser-synthesized febi nanoparticles for the efficient photocatalytic degradation of persistent antibiotics in water. *Journal of Water Process Engineering*. 2025, vol. 69, p. 106706.

[12] MORENO, José M., et al. Eco-friendly conductive hydrogels: towards green wearable electronics. *Gels*. 2025, vol. 11, no. 4.

[13] RAMAKRISHNAN, Rohith K., et al. Biomacromolecule assembly based on gum kondagogu-sodium alginate composites and their expediency in flexible packaging films. *International Journal of Biological Macromolecules*. 2021, vol. 177, p. 526-534.

[14] BEAUMONT, Marco, et al. Hydrogel-forming algae polysaccharides: from seaweed to biomedical applications. *Biomacromolecules*. 2021, vol. 22, no. 3.

[15] ZHANG, Baowei, et al. Thermally-induced reversible structural isomerization in colloidal semiconductor cds magic-size clusters. *Nature Communications*. 2018, vol. 9, no. 1.

[16] ABDUL KHALIL, H. P. S., et al. Preparation and characterization of modified and unmodified carrageenan based films. In: *IOP Conference Series: Materials Science and Engineering*. IOP Publishing, 2018. p. 012020.

[17] VDE. *Nuovo standard ICT 62368-1*. [online]. 2023. [viewed: 2025-08-22]. Available from: https://www.vde.com/tic-it/industries/information-technology/new-ict-standard

[18] U.S. Department of Agriculture. Food Safety and Inspection Service. [online]. 2025. [viewed: 2025-08-23]. Available from: https://www.fsis.usda.gov/

[19] MARTINS, Joana T., et al. Synergistic effects between κ-carrageenan and locust bean gum on physicochemical properties of edible films made thereof. *Food Hydrocolloids*. 2012, vol. 29, no. 2, pp. 280-289.